

# Diffusion Model-Augmented Behavioral Cloning

Hsiang-Chun Wang<sup>1</sup> Shang-Fu Chen<sup>1</sup> Shao-Hua Sun<sup>1</sup>

## Abstract

Imitation learning addresses the challenge of learning by observing an expert’s demonstrations without access to reward signals from the environment. Behavioral cloning (BC) formulates imitation learning as a supervised learning problem and learns from sampled state-action pairs. Despite its simplicity, it often fails to capture the temporal structure of the task and the global information of expert demonstrations. This work aims to augment BC by employing diffusion models for modeling expert behaviors, and designing a learning objective that leverages learned diffusion models to guide policy learning. To this end, we propose diffusion model-augmented behavioral cloning (Diffusion-BC) that combines our proposed diffusion model guided learning objective with the BC objective, which complements each other. Our proposed method outperforms baselines or achieves competitive performance in various continuous control domains, including navigation, robot arm manipulation, and locomotion. Ablation studies justify our design choices and investigate the effect of balancing the BC and our proposed diffusion model objective.

## 1 Introduction

Recently, the success of deep reinforcement learning (DRL) (Mnih et al., 2015; Lillicrap et al., 2016; Arulkumar et al., 2017) has inspired the research community to develop DRL frameworks to control robots, aiming to automate the process of designing sensing, planning, and control algorithms by letting the robot learn in an end-to-end fashion. However, acquiring complex skills through trial and error can still lead to undesired behaviors even with sophisticated reward design (Christiano et al., 2017; Leike et al., 2018). Moreover, the exploring process could damage expensive robotic platforms or even be dangerous

to humans (Garcia & Fernández, 2015; Levine et al., 2020).

To overcome this issue, imitation learning (*i.e.*, learning from demonstration) (Schaal, 1997; Osa et al., 2018) has received growing attention, whose aim is to learn a policy from a given set of expert demonstrations, which is often more accessible than appropriate reward functions for reinforcement learning. Among various imitation learning directions, adversarial imitation learning (Ho & Ermon, 2016; Zolna et al., 2021; Kostrikov et al., 2019) and inverse reinforcement learning (Ng & Russell, 2000; Abbeel & Ng, 2004) have achieved encouraging results in a variety of domains. Yet, these methods require interacting with environments, which can still be expensive or unsafe.

This work is interested in developing an imitation learning method that does not require interacting with environments, such as behavioral cloning (BC) (Pomerleau, 1989; Bain & Sammut, 1995). BC formulates imitation learning as a supervised learning problem — given an expert demonstration dataset, an agent policy takes states sampled from the dataset as input and learns to replicate the expert’s action. Due to its simplicity and effectiveness, BC has been widely adopted for visuomotor skill learning and autonomous driving. However, BC learns from decorrelated sampled state-action pairs, and often fails to capture the temporal structure of the task and the global information of expert demonstrations (Codevilla et al., 2019; Shafiullah et al., 2022).

In this work, we aim to augment BC by providing guidance that captures the temporal structure and global information of expert demonstrations. Our key insight is to employ diffusion models for modeling expert’s behaviors, and design a learning objective that leverages learned diffusion models to guide policy learning. As such, the BC objective directly guides the policy to replicate the expert’s action from sampled state-action pairs, while the diffusion model objective implicitly encourages the policy to mimic the expert behaviors by providing an estimate of how well the predicted action aligned with the global distribution of expert demonstrations. Our proposed method, diffusion model-augmented behavioral cloning (Diffusion-BC), combines the two complementary objectives.

We evaluate our proposed method and baselines in various continuous control domains, including navigation, robot arm manipulation, and locomotion. The experimental results

<sup>1</sup>National Taiwan University, Taipei, Taiwan. Correspondence to: Shao-Hua Sun <shaohuas@ntu.edu.tw>.

show that the proposed method outperforms all the baselines or achieves competitive performance in all tasks. Extensive ablation study compares our proposed method to its variants, justifying our design choices and investigating the effect of hyperparameters.

## 2 Related Work

Imitation learning (IL) addresses the challenge of learning by observing an expert’s demonstrations without access to reward signals from the environment. It has various applications such as robotics (Schaal, 1997), autonomous driving (Ly & Akhloufi, 2020), and game AI (Harmer et al., 2018). Most IL methods can be categorized into behavioral cloning, adversarial imitation learning, and inverse reinforcement learning.

**Behavioral Cloning (BC).** BC (Pomerleau, 1989; Bain & Sammut, 1995; Torabi et al., 2018a; Florence et al., 2022) formulate imitating an expert as a supervised learning problem. Due to its simplicity and effectiveness, it has been widely adopted in various domains. Yet, it can suffer from compounding errors caused by covariate shifts (Ross et al., 2011) since it learns from decorrelated state-action pairs. In this work, we aim to augment BC by employing a diffusion model that learns to model the expert’s demonstrations, designed to provide global information of the expert state-action pair distributions.

**Adversarial Imitation Learning (AIL).** AIL methods aim to match the state-action distribution of the agent to that of the expert via adversarial training. Generative adversarial imitation learning (GAIL) (Ho & Ermon, 2016) and its extensions (Torabi et al., 2018b; Kostrikov et al., 2019; Zolna et al., 2021) resemble the idea of generative adversarial networks (Goodfellow et al., 2014), which trains a generator (*i.e.*, a learner policy) to imitate an expert’s behaviors and a discriminator to distinguish between the expert and the learner’s state-action pair distributions. While modeling state-action pair distributions often leads to satisfactory performance, adversarial learning can be unstable and inefficient (Chen et al., 2020). Moreover, AIL methods require online interaction with environments, which might not always be possible. In contrast, the goal of this work is to (1) adopt this concept of matching state-action distributions while avoiding adversarial learning, and (2) develop a method that can learn when interacting with environments is not possible.

**Inverse Reinforcement Learning (IRL).** IRL methods (Ng & Russell, 2000; Abbeel & Ng, 2004; Fu et al., 2018; Lee et al., 2021) are designed to infer the reward function that underlies the expert demonstrations and then learn a policy using the inferred reward function. This allows for learning tasks whose reward functions are difficult to

manually specify. However, due to its double-loop learning procedure, IRL methods are typically computationally expensive and time-consuming. Additionally, obtaining accurate estimates of the expert’s reward function can be difficult, especially when the expert’s behavior is non-deterministic or when the expert’s demonstrations are sub-optimal.

## 3 Preliminaries

In this section, we discuss the preliminaries and the motivation of our proposed method.

### 3.1 Imitation Learning

Without loss of generality, the reinforcement learning problem can be formulated as an infinite-horizon Markov decision process (MDP), which can be represented by a tuple  $M = (S, A, R, P, \rho, \gamma)$  with states  $S$ , actions  $A$ , reward function  $R(S, A) \in (0, 1)$ , transition distribution  $P(s' | s, a) : S \times A \times S \rightarrow [0, 1]$ , initial state distribution  $\rho$ , and discounted factor  $\gamma$ .

Based on the rewards or penalties received while interacting with the environment, the goal is to learn a policy  $\pi(\cdot | s)$  to maximize the expectation of the cumulative discounted return (*i.e.*, value function):  $V(\pi) = \mathbb{E}[\sum_{t=0}^T \gamma^t R(s_t, a_t) | s_0 \sim \rho(\cdot), a_t \sim \pi(\cdot | s_t), s_{t+1} \sim P(s_{t+1} | s_t, a_t)]$ , where  $T$  is the episode length.

Instead of interacting with the environment and receiving rewards, imitation learning aims to learn an agent policy from an expert demonstration dataset, containing  $M$  trajectories,  $D = \{\tau_1, \dots, \tau_M\}$ , where  $\tau_i$  represents a sequence of  $n_i$  state-action pairs  $\{s_1^i, a_1^i, \dots, s_{n_i}^i, a_{n_i}^i\}$ . This can be formulated as minimizing the difference between agent’s value function and expert’s value function:  $\min_{\pi} V(\pi^E) - V(\pi)$ .

### 3.2 Behavioral Cloning

To learn an agent policy  $\pi$ , the behavioral cloning (BC) framework directly estimates the expert policy  $\pi^E$  with maximum likelihood estimation (MLE). Given a state-action pair  $(s, a)$  sampled from the dataset  $D$ , BC optimizes:

$$\max_{\theta} \sum_{(s,a) \in D} \log(\pi_{\theta}(a|s)), \quad (1)$$

where  $\theta$  is the parameter of the policy.

Equivalently, BC minimizes the divergence between an agent’s  $\pi$  and an expert’s policy  $\pi^E$  (*i.e.*, policy matching) (Ke et al., 2020):

$$\min_{\pi \in \Pi} D_{KL}(\pi^E || \pi) = \mathbb{E}_{s \sim d^{\pi^E}} [D_{KL}(\pi^E(\cdot | s) || \pi(\cdot | s))]. \quad (2)$$

Yet, it can suffer from compounding errors caused by covariate shifts (Ross et al., 2011) since it learns from decorrelated state-action pairs instead of modeling the entire state-action distribution of the expert data.

### 3.3 State-Action Distribution Matching

To alleviate the issue of compounding error, adversarial imitation learning (AIL) (Ho & Ermon, 2016) and inverse reinforcement learning (IRL) (Ng & Russell, 2000; Abbeel & Ng, 2004) aim to reduce the discrepancy between an agent’s and expert’s state-action distribution using Jensen–Shannon (JS) divergence. Instead of viewing the policy solely as a visiting conditional distribution  $\pi(\cdot|s)$  on actions, it examines the state-action distribution caused by a policy. This distribution-matching formulation is the core of a collection of methods that are more resilient to distribution shifts. Despite their promising performance, AIL and IRL methods are typically computationally expensive and time-consuming due to its double-loop learning procedure. Moreover, AIL training is often unstable since it involves adversarial learning (Chen et al., 2020).

This motivates us to develop a method for matching an agent’s and an expert’s state-action visiting distribution (*i.e.*, occupancy measure) without a double-loop learning procedure or an adversarial learning process. Occupancy measure  $P_\pi(s, a)$  represents the probability of observing a state-action pair  $(s, a)$  when executing a policy. It can be formulated as following:

$$P_\pi(s, a) := (1 - \gamma) \sum_{t=0}^{\infty} \gamma^t \mathbb{P}(s_t = s, a_t = a). \quad (3)$$

Under certain conditions, there is a direct correlation between a policy and its state-action visiting distribution  $P_\pi(s, a)$  (Puterman, 2014), as shown in following formula:

$$V(\pi) = \frac{1}{1 - \gamma} \sum_{(s,a) \in S \times A} P_\pi(s, a) R(s, a). \quad (4)$$

This indicates that when the distance between the state-action visiting distributions of an agent policy and an expert policy is proportional to the imitation learning objective  $\min_{\pi} V(\pi^E) - V(\pi)$  described in Section 3.1.

Our goal is to augment BC by adopting this concept of matching the state-action visiting distributions of an agent and an expert, while avoiding double-loop or adversarial learning. To this end, we aim to explicitly model the distribution of expert demonstration and guide policy learning with the learned model. Specifically, we propose learning diffusion models for distribution modeling, as discussed in the following.

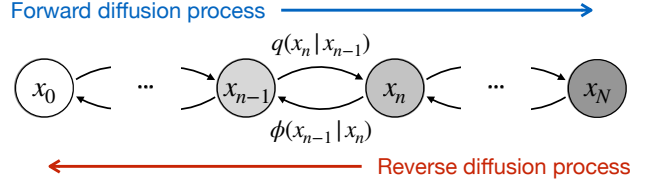


**Figure 1. Diffusion Model.** Latent variables  $x_1, \dots, x_N$  are produced from the data point  $x_0$  via the forward diffusion process, *i.e.*, gradually adding noises to the latent variables. The diffusion model  $\phi$  learns to reverse the diffusion process by denoising the noisy data to reconstruct the original data point  $x_0$ .

### 3.4 Diffusion Models

Generative models that can model data distributions such as generative adversarial networks (GANs) (Goodfellow et al., 2014), variational auto-encoder (VAEs) (Kingma & Welling, 2013), and flow-based models (Rezende & Mohamed, 2015; Dinh et al., 2017) have been used for various tasks, including image and video synthesis, sequence modeling, etc. Our goal is to leverage generative models to model expert’s state-action distribution and proposed an augmented behavioral cloning method.

GANs have been widely adopted in diverse domains, but adversarial training can be unstable and often produce limited diversity due to mode collapse and vanishing gradients (Che et al., 2016; Salimans et al., 2016; Huh et al., 2019). While VAEs have a solid theoretical foundation, the learning objective based on the difference between the input data and the reconstructed data is sensitive to the choice of architectures and hyperparameters (Bond-Taylor et al., 2021). Flow-based models can model high-dimensional, complicated data distributions and produce high-quality samples. Yet, they are computationally expensive, since they require computing complex invertible transformations (Kobyzev et al., 2020).

The diffusion model is a recently developed class of generative models, and has achieved encouraging results on various tasks (Sohl-Dickstein et al., 2015; Nichol & Dhariwal, 2021; Dhariwal & Nichol, 2021). Diffusion models use a Markov chain to convert noise distributions to data distributions. Unlike VAEs, diffusion models optimize likelihood-based objectives instead of reconstruction-based objectives, making the loss function directly related to the probability distribution of the data. This work explores using diffusion models for modeling expert state-action distributions and guiding policy learning.

Specifically, in this work, we utilize Denoising Diffusion Probabilistic Models (DDPMs) (J Ho, 2020), which recently achieves promising results in a wide range of domains, especially in image synthesis. DDPM models gradually add noise to authentic images until they become isotropic Gaus-

sian (*forward diffusion process*), and then learn to denoise each step and restore the original image (*reverse diffusion process*), as illustrated in Figure 1.

The forward diffusion process gradually adds Gaussian noise to the data in each  $n = 1, \dots, N$  step according to a pre-defined linear variance schedule  $\beta_1, \dots, \beta_N$ , which can be formulated as

$$q(x_n|x_{n-1}) := \mathcal{N}(x_n; \sqrt{1 - \beta_n}x_{n-1}, \beta_n \mathbf{I}), \quad (5)$$

and

$$q(x_{1:N}|x_0) := \prod_{n=1}^N q(x_n|x_{n-1}), \quad (6)$$

where  $q$  denotes the approximate posterior and  $x_1, \dots, x_N$  represent latent variables of the same size as the data point  $x_0 \sim q(x_0)$ .

The joint distribution  $\phi(x_{0:N})$  ( $\phi$  denotes the a diffusion model) can be obtained by learning the reverse diffusion process, which is defined as a Markov chain with learned Gaussian transitions initiating with  $p(x_N) = \mathcal{N}(x_N; \mathbf{0}, \mathbf{I})$ :

$$\phi(x_{n-1}|x_n) := \mathcal{N}(x_{n-1}; \mu_\theta(x_n, n), \Sigma_\theta(x_n, n)), \quad (7)$$

and

$$\phi(x_{0:N}) := p(x_N) \prod_{n=1}^N \phi(x_{n-1}|x_n). \quad (8)$$

The reverse diffusion process can be optimized by maximizing the usual evidence lower bound on negative log-likelihood (NLL) in Eq. 7. Once trained, we can sample a latent variable  $x \sim \mathcal{N}(x_N; \mathbf{0}, \mathbf{I})$ , and then go through the reverse diffusion process, moving from the last time step to the first one (*i.e.*, gradually denoising the "noisy data"), to produce a generated data point.

## 4 Approach

Our goal is to augment behavioral cloning with diffusion models trained to model the expert's demonstrations. To this end, we propose first learning a diffusion model that can model the distribution of state-action pairs sampled from the demonstration dataset. Then, we propose to leverage the variational bound as an estimate of how likely a state-action pair belongs to the expert demonstration distribution. To learn an agent policy, we augment the behavioral cloning objective with this guidance obtained from the diffusion model, whose goal is to encourage the policy to produce actions which can be recognized by the diffusion model, together with states given to the policy. An overview of our proposed framework is illustrated in Figure 2 and we detail the algorithm in Algorithm 1.

In Section 4.1, we present how to learn diffusion models from expert demonstrations. Then, in Section 4.2, we propose a learning objective that leverages learned diffusion

models. Finally, Section 4.3 discusses how we can combine our proposed diffusion model objective and the behavioral cloning objective, allowing the two objectives to complement each other.

---

### Algorithm 1 Diffusion Model-Augmented Behavioral Cloning (Diffusion-BC)

---

**Input:** Expert's Demonstration Dataset  $D$

**Output:** Policy  $\pi$ .

- 1: Randomly initialize a diffusion model  $\phi$
  - 2: **for** each diffusion model iteration **do**
  - 3:   Sample  $(s, a)$  from  $D$
  - 4:   Sample noise level  $n$  from  $\{0, \dots, N\}$
  - 5:   Update  $\phi$  using  $L_{\text{diff}}$  from Eq. 9
  - 6: **end for**
  - 7: Randomly initialize a policy  $\pi$
  - 8: **for** each policy iteration **do**
  - 9:   Sample  $(s, a)$  from  $D$
  - 10:   Predict an action  $\hat{a}$  using  $\pi$  from  $s$ :  $\hat{a} \sim \pi(s)$
  - 11:   Compute  $L_{\text{BC}}$  using Eq. 10
  - 12:   Sample noise level  $n$  from  $\{0, \dots, N\}$
  - 13:   Compute  $L_{\text{diff}}^{\text{agent}}$  with  $(s, \hat{a})$  using Eq. 11
  - 14:   Compute  $L_{\text{diff}}^{\text{expert}}$  with  $(s, a)$  using Eq. 12
  - 15:   Compute  $L_{\text{DM}}$  using Eq. 13
  - 16:   Update  $\pi$  using  $L_{\text{total}}$  from Eq. 14
  - 17: **end for**
  - 18: **return**  $\pi$
- 

### 4.1 Learning Diffusion Models

We aim to learn a diffusion model  $\phi$  that can model the distribution of expert demonstrations  $D$ . To this end, we inject noises with various levels into sampled demonstrations and train a denoising diffusion probabilistic model (DDPM) (J Ho, 2020) (described in Section 3.4) to recognize the demonstrations by predicting the injected noises.

To model both states and actions of the expert, we propose to learn from state-action pairs. For simplicity, we concatenate the state-action pair  $(s, a)$  to formulate the latent variable  $x$  for the diffusion model  $\phi$ . Then, we inject noises  $\epsilon(n)$  on  $x$ , where  $n$  indicates the number of steps of the Markov procedure in the DDPM, which can be viewed as a variable of the level of noise. The goal of the diffusion model is to reverse the diffusion process (*i.e.*, denoise), yielding the learning objective:

$$\begin{aligned} \mathcal{L}_{\text{diff}} &= \|\hat{\epsilon}(s, a, n) - \epsilon(n)\|^2 \\ &= \|\phi(s, a, \epsilon(n)) - \epsilon(n)\|^2, \end{aligned} \quad (9)$$

where  $\hat{\epsilon}$  is the noise predicted by the diffusion model  $\phi$ .

By predicting the noises with various levels from the expert state-action pairs, the diffusion model learns to construct



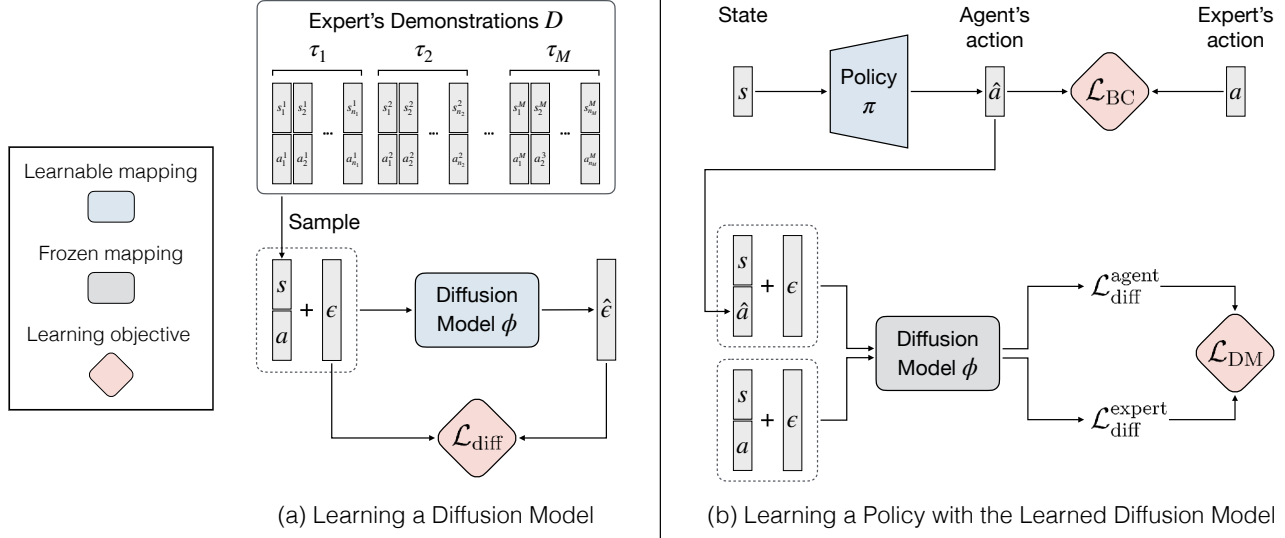


**Figure 2. Diffusion Model-Augmented Behavioral Cloning.** Our proposed method Diffusion-BC augments behavioral cloning (BC) by employing a diffusion model. (a) **Learning a Diffusion Model:** the diffusion model  $\phi$  learns to model the distribution of concatenated state-action pairs sampled from the demonstration dataset  $D$ . It learns to reverse the diffusion process (*i.e.*, denoise) by optimizing  $\mathcal{L}_{\text{diff}}$  in Eq. 9. (b) **Learning a Policy with the Learned Diffusion Model:** we propose a diffusion model objective  $\mathcal{L}_{\text{DM}}$  for policy learning and jointly optimize it with the BC objective  $\mathcal{L}_{\text{BC}}$ . Specifically,  $\mathcal{L}_{\text{DM}}$  is computed based on processing a sampled state-action pair  $(s, a)$  and a state-action pair  $(s, \hat{a})$  with the action  $\hat{a}$  predicted by the policy  $\pi$  with  $\mathcal{L}_{\text{diff}}$ .

the distribution of the demonstration dataset and therefore contains global information about expert behaviors. As a result, the diffusion model can serve as a reliable guide for the following behavioral cloning process.

## 4.2 Learning a Policy with the Learned Diffusion Model

Our goal is to utilize the learned diffusion model to guide the learning of our policy  $\pi$ , whose aim is to imitate expert behaviors. We adopt the behavioral cloning formulation, where the policy learns from a sampled state-action pair  $(s, a)$  by predicting an action  $\hat{a} \sim \pi(s)$ . We can optimize the policy by

$$\mathcal{L}_{\text{BC}} = d(a, \hat{a}), \quad (10)$$

where  $d(\cdot, \cdot)$  denotes a distance measure between a pair of actions. For example, we can adapt the mean-square error (MSE) loss  $\|a - \hat{a}\|^2$  for continuous control tasks.

While  $\mathcal{L}_{\text{BC}}$  provides direct supervision for the policy given each sample state-action pair  $(s, a)$ , it fails to capture the global information of the expert’s state-action distribution, as discussed in Section 3.2 and Section 3.3. Therefore, we propose to utilize the diffusion model to capture the distribution of the demonstration dataset and exploit it to assist the learning of our policy  $\pi$ .

Our key insight is to measure how well a state-action pair  $(s, a)$  aligns with the expert distribution by calculating the diffusion loss  $\mathcal{L}_{\text{diff}}$ . Intuitively, if the learned diffusion

model  $\phi$  can accurately predict the injected noise from the state-action pair, it is more likely that the pair is sampled from the expert distribution, and vice versa. The diffusion loss of the state-action pair with the predicted action  $(s, \hat{a})$  can be computed by the following equations:

$$\mathcal{L}_{\text{diff}}^{\text{agent}} = \|\hat{\epsilon}(s, \hat{a}, n) - \epsilon\|^2. \quad (11)$$

By minimizing this objective, the policy  $\pi$  learns to mimic the expert’s behaviors. However, even the state-action pair with the predicted action  $(s, \hat{a})$  matches the ground truth state-action pair  $(s, a)$ , if  $(s, a)$  is rarely seen in the expert distribution,  $\mathcal{L}_{\text{diff}}^{\text{agent}}$  can still be large. Therefore, we propose to address the above problem by normalizing the agent diffusion loss with an expert diffusion loss, which can be computed with expert state-action pair  $(s, a)$  as follows:

$$\mathcal{L}_{\text{diff}}^{\text{expert}} = \|\hat{\epsilon}(s, a, n) - \epsilon\|^2. \quad (12)$$

As such, a rarely seen  $(s, a)$  would yield large  $\mathcal{L}_{\text{diff}}^{\text{expert}}$ . By calculating the difference between the above agent and expert losses, we can alleviate the biases resulting from minor state-action pairs. Hence, our proposed diffusion model objective for policy learning is designed as follows:

$$\mathcal{L}_{\text{DM}} = \max(\mathcal{L}_{\text{diff}}^{\text{agent}} - \mathcal{L}_{\text{diff}}^{\text{expert}}, 0). \quad (13)$$

Optimizing the above objective encourages the policy to imitate the demonstrations’ global behaviors and can lead to more robust performance compared to behavioral cloning.

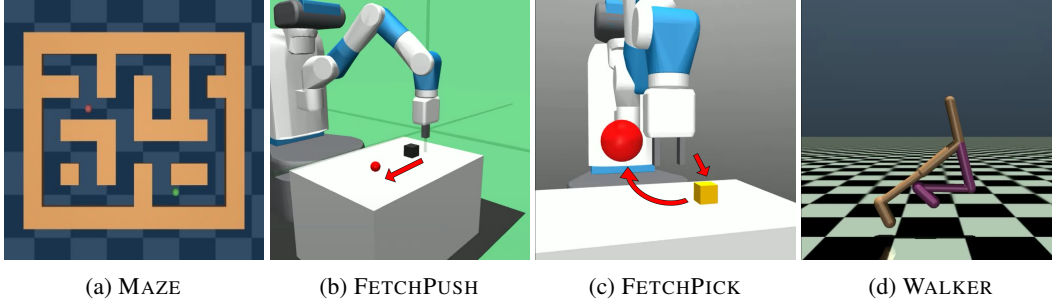


Figure 3. **Environments & Tasks.** (a) **MAZE**: a point-mass agent (green) in a 2D maze learns to navigate from its start location to a goal location (red) by iteratively predicting its  $x$  and  $y$  velocity. (b)-(c) **FETCHPUSH** and **FETCHPICK**: in robot arm manipulation tasks, a 7-DoF Fetch robotics arm is used. **FETCHPUSH** requires the arm to push an object (black cube) to a target location (red); **FETCHPICK** requires picking up an object (yellow cube) from the table and moving it to a target location (red). (d) **WALKER**: this locomotion task requires learning a bipedal walker policy to walk as fast as possible while maintaining its balance.

### 4.3 Combining the Two Objectives

The previous section presents two learning objectives for learning a policy  $\pi$  from demonstrations. While  $\mathcal{L}_{BC}$  in Eq. 10 directly guides the policy to replicate the expert’s action from sampled state-action pair,  $\mathcal{L}_{DM}$  in Eq. 13 implicitly encourages the policy to mimic the expert behaviors by providing an estimate of how well the predicted action aligned with the global distribution of demonstrations. To learn from both the two complementary objectives, we train the policy to optimize the following objective:

$$\mathcal{L}_{\text{total}} = \lambda_{BC}\mathcal{L}_{BC} + \lambda_{DM}\mathcal{L}_{DM}, \quad (14)$$

where  $\lambda_{BC}$  and  $\lambda_{DM}$  are coefficients that determine the importance of each objective. We design experiments and discuss the effect of the coefficients in Section 5.4.1.

## 5 Experiments

We design experiments in various continuous control domains, including navigation, robot arm manipulation, and locomotion, to compare our proposed method (Diffusion-BC) to its variants and baselines.

### 5.1 Experimental Setup

This section describes the environments, tasks, and expert demonstrations used for evaluation. More details can be found in Section A.

**Navigation.** To evaluate our method on a navigation task, we choose MAZE, a maze environment proposed in (Fu et al., 2020) (maze2d-medium-v1), as illustrated in Figure 3(a). This task features a point-mass agent in a 2D maze learning to navigate from its start location to a goal location by iteratively predicting its  $x$  and  $y$  velocity. The agent’s beginning and final locations are chosen randomly. We collect 100 demonstrations with 18,525 transitions using a controller.

**Robot Arm Manipulation.** We evaluate our method in a robot arm manipulation domain with two 7-DoF Fetch tasks: **FETCHPUSH** and **FETCHPICK**, as illustrated in Figure 3(b)-(c). **FETCHPUSH** requires the arm to push an object to a target location; **FETCHPICK** requires picking up an object from the table and lift it to a target location. We use the demonstrations provided in Lee et al. (2021) for these tasks. Each dataset contains 10k transitions (325 trajectories for **FETCHPUSH** and 303 trajectories for **FETCHPICK**).

**Locomotion.** For locomotion, we leverage the **WALKER** environment (Brockman et al., 2016), which requires a bipedal agent to walk as fast as possible while maintaining its balance, as illustrated in Figure 3(d). We use the demonstrations provided by Kostrikov (2018), which contains 53 trajectories, with around 50k state-action pairs.

### 5.2 Baselines

We compare our method Diffusion-BC with two baselines. **BC** directly learns to replicate the expert’s action from sample state-action pairs by optimizing  $\mathcal{L}_{BC}$  in Eq. 10.

To justify our choice of generative models (*i.e.*, diffusion models), we design another baseline, Variational Autoencoder-Augmented BC (**VAE-BC**), which learns a VAE to model the distribution of expert demonstrations. The objective of VAE is as follows:

$$\mathcal{L}_{\text{vae}} = ||\hat{x} - x||^2 + D_{\text{KL}}(\mathcal{N}(\mu_x, \sigma_x) || \mathcal{N}(0, 1)), \quad (15)$$

where  $x$  is the latent variable and  $\hat{x}$  is the reconstruction of  $x$ . The first term is the reconstruction loss, while the second term encourages aligning the data distribution with a normal distribution  $\mathcal{N}(0, 1)$ , where  $\mu_x$  and  $\sigma_x$  are the predicted mean and standard deviation given  $x$ . Once learned, how well a state-action pair fits the expert distribution should be reflected in the reconstruction loss. Hence, we design  $\mathcal{L}_{\text{VAE}} = \max(\mathcal{L}_{\text{vae}}^{\text{agent}} - \mathcal{L}_{\text{vae}}^{\text{expert}}, 0)$ , similar to Eq. 13. Then, VAE-BC optimizes  $\lambda_{BC}\mathcal{L}_{BC} + \lambda_{\text{VAE}}\mathcal{L}_{\text{VAE}}$ , similar to Eq. 14.

**Table 1. Experimental Result and Ablation Study.** We report the mean and the standard deviation of the success rate ( $\uparrow$ ), episode length ( $\downarrow$ ), and return ( $\uparrow$ ) on MAZE, FETCHPUSH, FETCHPICK, and WALKER, evaluated over three random seeds. The experimental demonstrates that our proposed method (Diffusion-BC) outperforms the baselines on MAZE, FETCHPUSH, FETCHPICK and performs competitively against the baselines on WALKER.

Method	MAZE		FETCHPUSH		FETCHPICK		WALKER Return
	Success Rate	Episode Length	Success Rate	Episode Length	Success Rate	Episode Length	
BC	78.58% $\pm$ 4.09%	214.67 $\pm$ 3.95	52.94% $\pm$ 8.16%	47.54 $\pm$ 0.48	56.18% $\pm$ 17.20%	41.01 $\pm$ 2.64	<b>7067.1</b> $\pm$ 21.3
VAE-BC	78.92% $\pm$ 7.93%	221.65 $\pm$ 16.47	54.22% $\pm$ 7.76%	47.41 $\pm$ 0.47	59.51% $\pm$ 18.45%	40.48 $\pm$ 2.83	7059.9 $\pm$ 30.7
Diffusion-BC	<b>86.86%</b> $\pm$ 3.32%	<b>203.47</b> $\pm$ 6.26	<b>69.42%</b> $\pm$ 10.70%	<b>46.16</b> $\pm$ 0.76	<b>67.83%</b> $\pm$ 11.95%	<b>38.31</b> $\pm$ 1.91	7047.8 $\pm$ 58.1

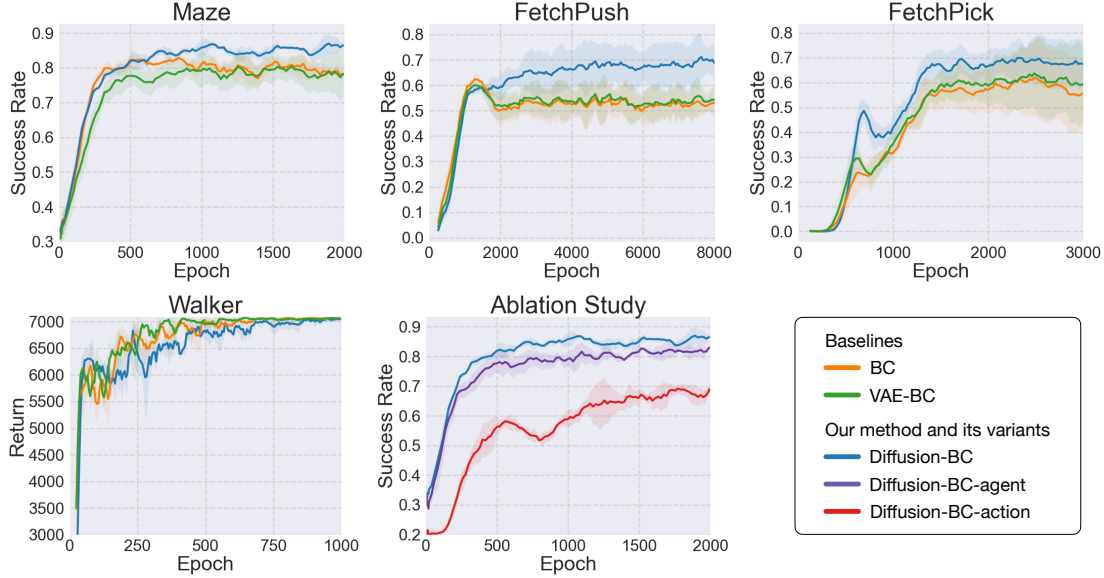


**Figure 4. Learning Progress.** We evaluate the baselines and our proposed method and its variants during the learning process. Our method (Diffusion-BC in blue) demonstrates superior learning efficiency and is more robust to overfitting. The ablation study shows that our method learning from state-action pairs with the normalizing term ( $\mathcal{L}_{diff}^{expert}$ ) achieves the best performance, justifying our design.

where  $(\lambda_{BC}, \lambda_{VAE})$  is set to  $(1, 1)$  as discussed in Section 5.4.1. The performance of VAE-BC should justify choosing diffusion models to model expert demonstrations.

### 5.3 Experimental Results

We report the experimental results in terms of success rate (MAZE, FETCHPUSH, FETCHPICK), episode length (MAZE, FETCHPUSH, FETCHPICK), and return (WALKER) in Table 1. We evaluate the baselines and our method during the learning process, and present it in Figure 4. All experiments are evaluated with the model from the last training epoch over 100 episodes with three random seeds.

**Navigation & Robot Arm Manipulation.** Our proposed method Diffusion-BC achieves the highest success rates, outperforming BC and VAE-BC by a large margin in MAZE, FETCHPUSH, and FETCHPICK. Moreover, Diffusion-BC produces shorter trajectories, indicating that our method learns a more efficient policy.

The result is expected since the agent needs to capture long-

term/global information of the expert demonstrations for learning these goal-directed tasks. However, the BC objective only considers a state-action pair at each training iteration, so it tends to act aggressively at each time step and leads to inferior success rates. While VAE-BC attempts to model the global distribution of the expert demonstrations with a VAE by learning to reconstruct, the result suggests that it might not be suitable for policy learning.

In contrast, the expert distribution is well captured by our diffusion model, which can augment BC and guide policy learning with our designed objective. The learning progress reported in Figure 4(a)-(c) further verify the above statement. One can observe that BC and VAE-BC learn quickly in the early training stage but are stuck in a local minimum and then overfit afterward, while Diffusion-BC learns steadily and converges to better success rates.

**Locomotion.** Unlike the above three tasks, we do not observe significant improvement but competitive results from Diffusion-BC compared to BC and VAE-BC. We hypothesize that this is because locomotion tasks such as WALKER

Table 2. **Effect of the Coefficients  $\lambda_{BC}$  and  $\lambda_{DM}$ .** We experiment with different values of  $\lambda_{BC}$  and  $\lambda_{DM}$  on MAZE. Each coefficient set is evaluated over three random seeds. Setting  $\lambda_{BC} = 1$  and  $\lambda_{DM} = 1$  achieves the best performance.

Coefficient		Success Rate	Episode Length
$\lambda_{BC}$	$\lambda_{DM}$		
1	0.2	82.54% $\pm$ 3.75%	204.57 $\pm$ 2.44
1	1	<b>86.69%</b> $\pm$ 2.77%	202.48 $\pm$ 3.71
1	5	84.11% $\pm$ 2.70%	<b>200.16</b> $\pm$ 4.77
1	10	81.64% $\pm$ 4.45%	207.65 $\pm$ 3.66
0	1	54.13% $\pm$ 2.49%	250.95 $\pm$ 5.68

do not require modeling global information of the expert demonstrations; instead, a policy can simply follow the direct supervision provided by the BC objective.

#### 5.4 Ablation Study

We compare our proposed method to its variants to justify our design choices and investigate the effect of hyperparameters in MAZE.

##### 5.4.1 Effect of the Coefficients $\lambda_{BC}$ and $\lambda_{DM}$

We examined the impact of varying the coefficients of the two learning objectives in Eq. 14:  $\lambda_{BC}$  for  $\mathcal{L}_{BC}$  and  $\lambda_{DM}$  for  $\mathcal{L}_{DM}$ . The result is presented in Table 2. We find that setting  $(\lambda_{BC}, \lambda_{DM}) = (1, 1)$  yields the highest success rate and performs competitively in terms of episode length (within one standard deviation). A higher or lower coefficient ratio  $\lambda_{BC}/\lambda_{DM}$  results in worse performance, demonstrating how the two learning objectives can complement each other by combining direct supervision ( $\mathcal{L}_{BC}$ ) and global information of expert distributions ( $\mathcal{L}_{DM}$ ).

##### 5.4.2 Effect of the Normalization Term $\mathcal{L}_{diff}^{expert}$

We discuss how normalizing the diffusion loss of the agent state-action pair  $(s, \hat{a})$  with the expert pair  $(s, a)$  can alleviate the biases resulting from minor expert state-action pairs in Section 4.2. We examine the effectiveness of this design by evaluating a variant of our method, dubbed Diffusion-BC-agent, where only  $\mathcal{L}_{diff}^{agent}$  in Eq. 11 is used to augment BC instead of  $\mathcal{L}_{DM}$  in Eq. 13. We present the quantitative result in Table 3 and visual the learning progress in Figure 4. Diffusion-BC outperforms Diffusion-BC-agent in terms of success rate with competitive episode length (within one standard deviation). This verifies the effectiveness of the proposed normalization term  $\mathcal{L}_{diff}^{expert}$  in Eq. 13.

##### 5.4.3 Learning Diffusion Model from Expert Actions

This work proposes to model the expert state-action distribution by learning a diffusion model from concatenated state-

Table 3. **Ablation Study.** We justify our design choices in MAZE.

Method	Success Rate	Episode Length
Diffusion-BC-action	67.37% $\pm$ 1.34%	218.45 $\pm$ 7.54
Diffusion-BC-agent	82.27% $\pm$ 1.22%	<b>200.08</b> $\pm$ 4.43
Diffusion-BC	<b>86.86%</b> $\pm$ 3.32%	203.47 $\pm$ 6.26

action pairs. We examine the effectiveness of this design by evaluating a variant of our method, dubbed Diffusion-BC-action, whose diffusion model only learns from actions in expert demonstrations. The result is presented in Table 3 and Figure 4. Diffusion-BC significantly outperforms Diffusion-BC-action in terms of both success rate and episode length. This confirms the effectiveness of learning a diffusion model from the expert state-action pairs.

Please refer to Section B for model architecture designs and Section C for training details. Additional analysis and experimental results can be found in Section D.

## 6 Discussion

We propose diffusion model-augmented behavioral cloning (Diffusion-BC) to augment BC. Specifically, we employ diffusion models for modeling expert behaviors, and design a learning objective that leverages learned diffusion models to guide policy learning. Then, our full objective combines the BC objective, which directly guides the policy to replicate the expert’s action from sampled state-action pairs, and the diffusion model objective, which implicitly encourages the policy to mimic expert behaviors by providing an estimate of how well the predicted action aligned with the global distribution of expert demonstrations. Our proposed method outperforms baselines or achieves competitive performance in various continuous control tasks in navigation, robot arm manipulation, and locomotion. Ablation studies verify the effectiveness of our design choices and investigate the effect of hyperparameters.

In the following, we discuss the limitation of the proposed method. First, our method learns a policy relying on a diffusion model that learns to model expert demonstrations. As a result, our method is not expected to yield improved performance when diffusion models struggle at learning from expert demonstrations. Specifically, Austin et al. (2021); Kotelnikov et al. (2022) reported that DDPMs perform poorly for modeling discrete random variables (*e.g.* text). Hence, we hypothesize that our method might not be suitable for learning to model demonstrations with discrete states or actions. Second, our proposed method in its current form is not able to learn from trajectories produced by the agent policy. Extending our method to incorporate agent data can allow for improvement when online interacting environments is possible, which is left for future work.



## References

- Abbeel, P. and Ng, A. Y. Apprenticeship learning via inverse reinforcement learning. In *International Conference on Machine Learning*, 2004.
- Arulkumaran, K., Deisenroth, M. P., Brundage, M., and Bharath, A. A. Deep reinforcement learning: A brief survey. *IEEE Signal Processing Magazine*, 2017.
- Austin, J., Johnson, D. D., Ho, J., Tarlow, D., and van den Berg, R. Structured denoising diffusion models in discrete state-spaces. *Advances in Neural Information Processing Systems*, 2021.
- Bain, M. and Sammut, C. A framework for behavioural cloning. In *Machine Intelligence 15*, 1995.
- Bond-Taylor, S., Leach, A., Long, Y., and Willcocks, C. G. Deep generative modelling: A comparative review of vaes, gans, normalizing flows, energy-based and autoregressive models. *IEEE Transactions on Pattern Analysis and Machine Intelligence*, 2021.
- Brockman, G., Cheung, V., Pettersson, L., Schneider, J., Schulman, J., Tang, J., and Zaremba, W. Openai gym, 2016.
- Che, T., Li, Y., Jacob, A. P., Bengio, Y., and Li, W. Mode regularized generative adversarial networks. *arXiv preprint arXiv:1612.02136*, 2016.
- Chen, M., Wang, Y., Liu, T., Yang, Z., Li, X., Wang, Z., and Zhao, T. On computation and generalization of generative adversarial imitation learning. In *International Conference on Learning Representations*, 2020.
- Christiano, P. F., Leike, J., Brown, T., Martic, M., Legg, S., and Amodei, D. Deep reinforcement learning from human preferences. In *Advances in Neural Information Processing Systems*, 2017.
- Codevilla, F., Santana, E., López, A. M., and Gaidon, A. Exploring the limitations of behavior cloning for autonomous driving. In *International Conference on Computer Vision*, 2019.
- Dhariwal, P. and Nichol, A. Diffusion models beat gans on image synthesis. *Neural Information Processing Systems*, 2021.
- Dinh, L., Sohl-Dickstein, J., and Bengio, S. Density estimation using real NVP. In *International Conference on Learning Representations*, 2017.
- Florence, P., Lynch, C., Zeng, A., Ramirez, O. A., Wahid, A., Downs, L., Wong, A., Lee, J., Mordatch, I., and Tompson, J. Implicit behavioral cloning. In *Conference on Robot Learning*, 2022.
- Fu, J., Luo, K., and Levine, S. Learning robust rewards with adversarial inverse reinforcement learning. In *International Conference on Learning Representations*, 2018.
- Fu, J., Kumar, A., Nachum, O., Tucker, G., and Levine, S. D4rl: Datasets for deep data-driven reinforcement learning. *arXiv preprint arXiv:2004.07219*, 2020.
- Garcia, J. and Fernández, F. A comprehensive survey on safe reinforcement learning. *Journal of Machine Learning Research*, 2015.
- Goodfellow, I., Pouget-Abadie, J., Mirza, M., Xu, B., Warde-Farley, D., Ozair, S., Courville, A., and Bengio, Y. Generative adversarial nets. In *Advances in Neural Information Processing Systems*, 2014.
- Harmer, J., Gisslén, L., del Val, J., Holst, H., Bergdahl, J., Olsson, T., Sjöö, K., and Nordin, M. Imitation learning with concurrent actions in 3d games. In *IEEE Conference on Computational Intelligence and Games*. IEEE, 2018.
- Ho, J. and Ermon, S. Generative adversarial imitation learning. In *Advances in Neural Information Processing Systems*, 2016.
- Huh, M., Sun, S.-H., and Zhang, N. Feedback adversarial learning: Spatial feedback for improving generative adversarial networks. In *Proceedings of IEEE Conference on Computer Vision and Pattern Recognition (CVPR)*, 2019.
- J Ho, A. J. Denoising diffusion probabilistic models. In *Advances in Neural Information Processing Systems*, 2020.
- Ke, L., Choudhury, S., Barnes, M., Sun, W., Lee, G., and Srinivasa, S. Imitation learning as f-divergence minimization. In *International Workshop on the Algorithmic Foundations of Robotics*, 2020.
- Kingma, D. P. and Welling, M. Auto-encoding variational bayes. *arXiv preprint arXiv:1312.6114*, 2013.
- Kobyzev, I., Prince, S. J., and Brubaker, M. A. Normalizing flows: An introduction and review of current methods. *IEEE Transactions on Pattern Analysis and Machine Intelligence*, 2020.
- Kostrikov, I. Pytorch implementations of reinforcement learning algorithms. <https://github.com/ikostrikov/pytorch-a2c-ppo-acktr-gail>, 2018.
- Kostrikov, I., Agrawal, K. K., Dwibedi, D., Levine, S., and Tompson, J. Discriminator-actor-critic: Addressing sample inefficiency and reward bias in adversarial imitation learning. In *International Conference on Learning Representations*, 2019.

- Kotelnikov, A., Baranchuk, D., Rubachev, I., and Babenko, A. Tabddpm: Modelling tabular data with diffusion models. *arXiv preprint arXiv:2209.15421*, 2022.
- Lee, Y., Szot, A., Sun, S.-H., and Lim, J. J. Generalizable imitation learning from observation via inferring goal proximity. In *Neural Information Processing Systems*, 2021.
- Leike, J., Krueger, D., Everitt, T., Martic, M., Maini, V., and Legg, S. Scalable agent alignment via reward modeling: a research direction. *arXiv preprint arXiv:1811.07871*, 2018.
- Levine, S., Kumar, A., Tucker, G., and Fu, J. Offline reinforcement learning: Tutorial, review, and perspectives on open problems. *arXiv preprint arXiv:2005.01643*, 2020.
- Lillicrap, T. P., Hunt, J. J., Pritzel, A., Heess, N., Erez, T., Tassa, Y., Silver, D., and Wierstra, D. Continuous control with deep reinforcement learning. In *International Conference on Learning Representations*, 2016.
- Ly, A. O. and Akhloufi, M. Learning to drive by imitation: An overview of deep behavior cloning methods. *IEEE Transactions on Intelligent Vehicles*, 2020.
- Mnih, V., Kavukcuoglu, K., Silver, D., Rusu, A. A., Veness, J., Bellemare, M. G., Graves, A., Riedmiller, M., Fidjeland, A. K., Ostrovski, G., et al. Human-level control through deep reinforcement learning. *Nature*, 2015.
- Ng, A. Y. and Russell, S. J. Algorithms for inverse reinforcement learning. In *International Conference on Machine Learning*, 2000.
- Nichol, A. Q. and Dhariwal, P. Improved denoising diffusion probabilistic models. In *International Conference on Machine Learning*, 2021.
- Osa, T., Pajarinen, J., Neumann, G., Bagnell, J. A., Abbeel, P., Peters, J., et al. An algorithmic perspective on imitation learning. *Foundations and Trends® in Robotics*, 2018.
- Pomerleau, D. A. Alvin: An autonomous land vehicle in a neural network. In *Advances in Neural Information Processing Systems*, 1989.
- Puterman, M. L. *Markov decision processes: discrete stochastic dynamic programming*. John Wiley & Sons, 2014.
- Rezende, D. and Mohamed, S. Variational inference with normalizing flows. In *International Conference on Machine Learning*, 2015.
- Ross, S., Gordon, G., and Bagnell, D. A reduction of imitation learning and structured prediction to no-regret online learning. In *International Conference on Artificial Intelligence and Statistics*, 2011.
- Salimans, T., Goodfellow, I., Zaremba, W., Cheung, V., Radford, A., and Chen, X. Improved techniques for training gans. *Advances in neural information processing systems*, 29, 2016.
- Schaal, S. Learning from demonstration. In *Advances in Neural Information Processing Systems*, 1997.
- Shafiullah, N. M. M., Cui, Z. J., Altanzaya, A., and Pinto, L. Behavior transformers: Cloning  $k$  modes with one stone. In *Neural Information Processing Systems*, 2022.
- Sohl-Dickstein, J., Weiss, E., Maheswaranathan, N., and Ganguli, S. Deep unsupervised learning using nonequilibrium thermodynamics. In *International Conference on Machine Learning*. PMLR, 2015.
- Torabi, F., Warnell, G., and Stone, P. Behavioral cloning from observation. In *International Joint Conference on Artificial Intelligence*, 2018a.
- Torabi, F., Warnell, G., and Stone, P. Generative adversarial imitation from observation. *arXiv preprint arXiv:1807.06158*, 2018b.
- Zolna, K., Reed, S., Novikov, A., Colmenarejo, S. G., Buden, D., Cabi, S., Denil, M., de Freitas, N., and Wang, Z. Task-relevant adversarial imitation learning. In *Conference on Robot Learning*, 2021.

## Appendix

### A Environment & Task Details

#### A.1 MAZE

A point-maze agent in a 2D maze learns to navigate from its start location to a goal location by iteratively predicting its x and y velocity. The agent’s beginning and final locations are chosen randomly. An episode terminates when the maximum episode length 400 is reached. We evaluate the agents with 100 episodes and three random seeds and compare the average success rate and episode lengths, representing the agents’ effectiveness and efficiency. The observed states include position, velocity, and goal position.

#### A.2 FETCHPUSH & FETCHPICK

FETCHPUSH requires the arm to push an object to a target location; FETCHPICK requires picking up an object from the table and moving it to a target location. An episode terminates when the agent completes the goal or the maximum episode length is reached, which is 50 in both environments. We evaluate the agents with 100 episodes and three random seeds and compare the average success rate and episode lengths, representing the agents’ effectiveness and efficiency.

Following the environment setups of [Lee et al. \(2021\)](#), the 16D state representation consists of the angles of the robot joints, the robot arm pose relative to the object, and goal positions. The first three dimensions of the action indicate the desired relative position at the next time step. For FETCHPICK, there is an additional action dimension to specify the distance between the two fingers of the gripper.

#### A.3 WALKER

WALKER requires an agent to walk toward x-coordinate as fast as possible while maintaining its balance. An episode terminates when the agent is unhealthy, i.e., ill conditions predefined in the environment, or the maximum episode length (1000) is reached. We evaluate the agent with 100 episodes and three random seeds and compare the average returns of episodes. The return of an episode is accumulated from all timesteps of the episode. The 17D state consists of angles of joints, angular velocities of joints, and velocities of the x and z-coordinate of the top. The 6D action specifies the torques to be applied on each joint of the walker avatar.

### B Model Architecture

All policy model  $\pi$  used in this paper consists of three linear layers. The input/output dimensions are equal to the state/action dimensions in each environment, and the dimension of the hidden layer is 256. For MAZE, the architecture of diffusion models is four linear layers and ReLU nonlinear activation, and the size of the hidden dimension is 128. As For FETCHPUSH, FETCHPICK, and WALKER, the architecture of diffusion models is five linear layers with a 0.2 dropout ratio, batch normalization, and ReLU nonlinear activation, and The size of the hidden dimension is 1024. The input/output dimensions are 8, 19, 20, and 23 for MAZE, FETCHPUSH, FETCHPICK, and WALKER, respectively, which is the summation of the state and action dimensions.

### C Training and Evaluation Details

For MAZE, the diffusion models are trained for 8,000 epochs with a learning rate of 0.0001. We set  $\lambda_1 = 1$  and  $\lambda_2 = 1$  and train the policy model for 2,000 epochs with a learning rate of 0.0001.

For FETCHPUSH, FETCHPICK, and WALKER, the diffusion models are trained for 10,000 epochs with a learning rate of 0.0001. We set  $\lambda_1 = 1$  and  $\lambda_2 = 0.2$  and train the policy model for 8,000 epochs with a learning rate of 0.000001 for FETCHPUSH. For FETCHPICK, we have  $\lambda_1 = 1$  and  $\lambda_2 = 0.1$  for and train the policy model for 4,000 epochs with a learning rate of 0.000002. Since we observe overfitting for all methods, we apply an early stop at 3,000 epochs. As for WALKER, we set  $\lambda_1 = 1$  and  $\lambda_2 = 5$  and train the policy model for 1,000 epochs with a learning rate of 0.0001. All optimizers used in this paper are Adam optimizers with linear learning rate decay schedulers.

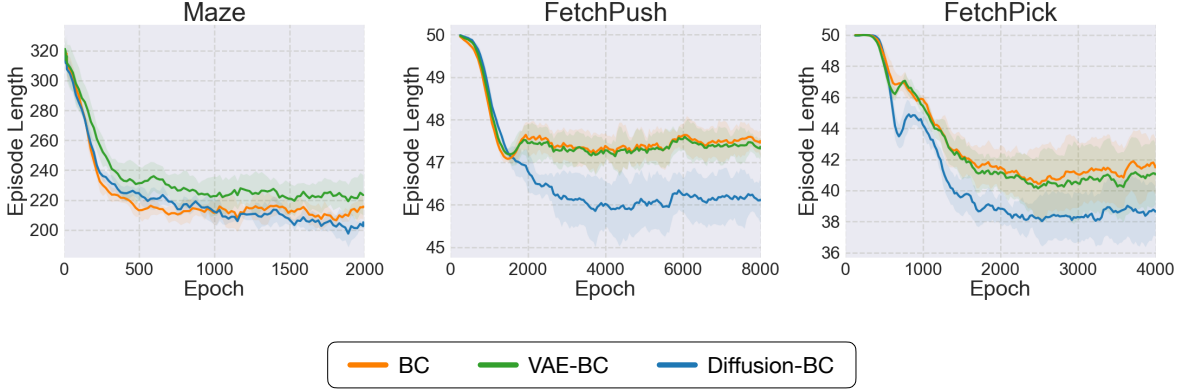


**Figure 5. Episode Length.** We evaluate the baselines and our proposed method regarding the episode length during the learning process. The average episode length indicates how fast the agent reaches the goal, which can be a measurement of the efficiency of the agent. Therefore, our method (Diffusion-BC in blue) demonstrates superior learning efficiency and is more robust to overfitting.

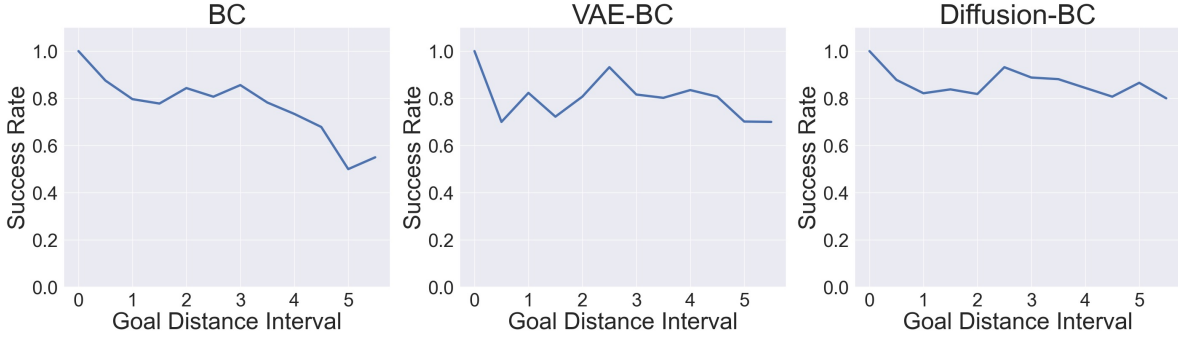


**Figure 6. Goal Distance Analysis.** We compare the success rates of the baselines and our proposed method regarding the distance between the start point and the goal. The success rates of BC and VAE-BC decrease significantly as the distance range increases, while the success rate of our method Diffusion-BC remains relatively consistent.

## D Additional Analysis and Qualitative Results

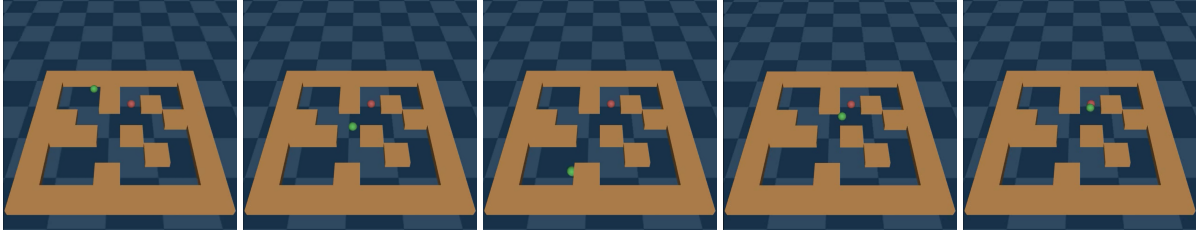
### D.1 Episode Length

In Figure 5, we compare our Diffusion-BC with BC and VAE-BC baselines regarding average episode lengths over 100 episodes and three random seeds. We observe that Diffusion-BC results in the shortest episode lengths in all environments since our method learns to mimic the expert demonstrations’ global behaviors implicitly with the guidance of the diffusion model. On the other hand, BC does not consider the global distribution of the demonstrations; VAE-BC is not able to model the distribution well via the reconstruction objective. The result indicates that Diffusion-BC can learn a more efficient agent than the two baselines.

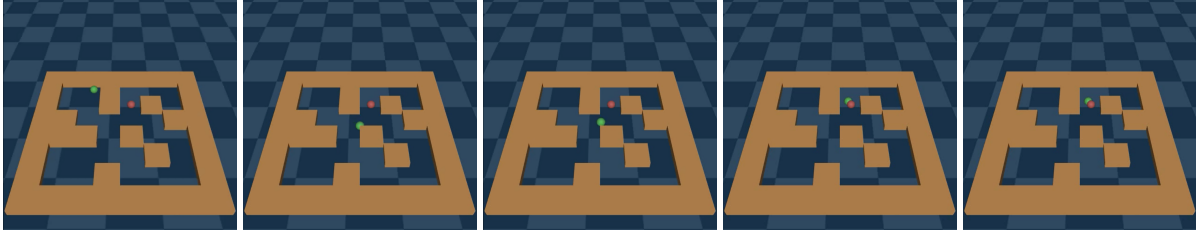
### D.2 Success Rate Analysis Regarding to Goal Distance

We compare the performance of our Diffusion-BC against BC and VAE-BC baselines with regard to the distance between the starting location and the goal in MAZE environment. The goal distance from the starting location measures the difficulty of the sampled MAZE tasks. When the goal distance becomes larger, the agent must take more steps to reach the goal and, therefore, is more likely to fail such a task in the limitation of the maximum episode length. We demonstrate the results in Figure 6. We see that the success rates of all methods are high when the goal distances are small. However, the success rate of the BC and VAE-BC agent decreased significantly as the goal distances increased. On the other hand, our Diffusion-BC performs more consistent results across different goal distances. The result verifies that the proposed method can capture the temporal structure of the task and therefore reaches harder goals with global information considered.

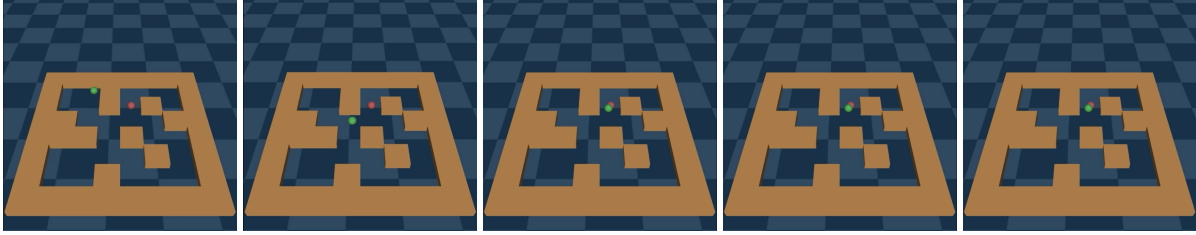




(a) BC



(b) VAE-BC



(c) Diffusion-BC

*Figure 7. Trajectories.* **BC**: the agent takes 365 steps to reach the goal. **VAE-BC**: the agent takes 252 steps to reach the goal. **Diffusion-BC**: the agent takes 181 steps to reach the goal. The above results justify the effectiveness of our proposed method against the baselines.

### D.3 Qualitative Visualizations

We visualize an episode to observe the behavior of our Diffusion-BC compared to BC and VAE-BC baseline in Figure 7. From the top to the bottom row, we show the trajectory of BC, VAE-BC, and Diffusion-BC, respectively. Our Diffusion-BC reaches the goal with the least steps (181), while BC and VAE-BC take more steps (252 and 365) to reach the same goal.